Rare Met.
https://doi.org/10.1007/s12598-021-01792-3

RARE METALS

LETTER

MgO intercalation and crystallization between epitaxial graphene and Ru(0001)

Xue-Yan Wang, Hui Guo, Jin-An Shi, Yi Biao, Yan Li, Guang-Yuan Han, Shuai Zhang, Kai Qian, Wu Zhou, Xiao Lin, Shi-Xuan Du, Cheng-Min Shen, Hong-Liang Lu*, Hong-Jun Gao

Received: 20 February 2021 / Revised: 6 April 2021 / Accepted: 23 April 2021

Graphene on insulator is the foundation of its practical applications in electronic information technology. However, fabrication of graphene on insulating substrates suffers from small size and limited quality by direct growth of graphene on dielectric substrates, and the method of transferring graphene onto insulating substrates is not so compatible with the large-scale production in industry. Here, we report the fabrication of high-quality, large-area, single-crystal graphene on crystalline magnesium oxide (MgO), which has a dielectric constant of 7–10. Magnesium and oxygen are intercalated at the interface of epitaxial graphene/Ru(0001) and form crystalline structure after high-temperature annealing. The graphene/MgO/Ru(0001) sample was characterized by low energy electron diffraction (LEED), scanning tunneling microscopy (STM), X-ray photoelectron spectroscopy (XPS), and scanning transmission electron microscopy (STEM). LEED pattern shows that the magnesium oxide displays crystalline structure, and STM studies show clearly that the top layer is graphene. STEM characterization of as-intercalated sample demonstrates that the MgO intercalation layer, with a thickness of up to 2.3 nm, has a crystal structure of rock salt MgO, and the out-of-plane crystal orientation is [001]. Our work provides a new route for fabrication of graphene on high dielectric constant insulators, which may have potential applications in future electronics.

Graphene (Gr) has attracted extensive attention because of its two-dimensional (2D) sp^2 hybridized honeycomb carbon lattice and excellent properties. The preparation of large-area uniform graphene with low defect density on insulating substrates is crucial for its comprehensive applications especially in electronics. Exfoliation from bulk graphite and transferring onto insulating substrates was proposed at the very beginning, but the size of graphene obtained by exfoliation is limited and this method has poor thickness controllability [1–3]. An alternative approach involves the transfer of graphene films synthesized on a catalytic metal substrate onto dielectric substrates. However, such transfer process inevitably produces defects that degrade the properties of the synthesized graphene [4–7]. Another possible route is to directly grow graphene layers on dielectric substrates [8–12]. However, graphene synthesized in such an approach always has a limited size and high defect density.

Epitaxial growth on transition metal single crystal surfaces [13–15] provides an effective way to fabricate high-quality, large-area graphene. However, the strong interaction between graphene and transition metal substrates, which arises from the hybridization of graphene's π bond with the d orbitals of metal atoms, destroys its unique electronic structure. Interestingly, previous works have shown that graphene/metal interface can be intercalated with other atoms [16], and the strong interaction between

Supplementary Information The online version contains supplementary material available at https://doi.org/10.1007/s12598-021-01792-3.

X.-Y. Wang, H. Guo, J.-A. Shi, Y. Biao, Y. Li, G.-Y. Han, S. Zhang, K. Qian, W. Zhou, X. Lin, S.-X. Du, C.-M. Shen, H.-L. Lu*, H.-J. Gao
Institute of Physics and University of Chinese Academy of Sciences, Chinese Academy of Sciences, Beijing 100190, China
e-mail: luhl@ucas.ac.cn

W. Zhou, X. Lin, S.-X. Du, C.-M. Shen, H.-L. Lu, H.-J. Gao
CAS Center for Excellence in Topological Quantum Computation, University of Chinese Academy of Sciences, Beijing 100190, China

S.-X. Du, H.-J. Gao
Songshan Lake Materials Laboratory, Dongguan 523808, China

Published online: 26 July 2021

graphene and metal substrates can be effectively suppressed by intercalation with atoms including Si [17], Hf [18], Pb [19], and Au [20]. Such intercalation could restore the linearly dispersed energy band of graphene [17–19] or even open up a band gap at the Dirac point [20]. Furthermore, via intercalation of silicon and oxygen, insulating SiO_2 layer can form between graphene and the metal substrate [21]. However, the thickness of the oxide layer is only about 1.8 nm, as estimated by XPS. And recently, GeO_x has been intercalated between graphene and the metal substrate, and the transport measurements demonstrate that GeO_x layer can act as a tunneling barrier in the heterostructure [22]. Besides, it was reported that for graphene grown on a bimetallic Ni_3Al alloy and subsequently exposed to oxygen at 520 K, a 1.5-nm-thick alumina nanosheet could form underneath graphene [23]. The successful intercalation of SiO_2, GeO_x and Al_2O_3 at the graphene–metal interface suggests the possibility of intercalating other oxides between graphene and metal substrates and increasing the thickness of the intercalated oxide. MgO has a high dielectric constant and an extremely wide band gap and can be used as an efficient tunnel barrier material for spin injection in graphene-based spintronic devices [24]. However, intercalation of MgO between graphene and metal substrates has rarely been realized.

In this article, we successively intercalated magnesium and oxygen between graphene and Ru(0001) surface using molecular beam epitaxy (MBE) and formed magnesium oxide by annealing. LEED and STEM characterizations demonstrate that a crystalline MgO intercalation layer with a thickness of up to $\sim$ 2.3 nm was formed after annealing. The intercalated MgO has an fcc structure as bulk MgO. Our results provide a new approach for the fabrication of graphene on magnesium oxide. The as-fabricated graphene/MgO/metal heterostructure holds potential applications in microelectronic devices based on high-quality and large-area graphene.

Our sample growth was performed in an ultra-high vacuum (UHV) MBE system equipped with a LEED, evaporators, an electron beam heater, and with a base pressure of 2.0×10^{-8} Pa. The Ru(0001) surface was prepared by a few cycles of Ar^+ sputtering and annealing. We grew high quality monolayer graphene by thermal decomposition of ethylene on the Ru(0001) substrate at 1030 °C, which was measured by infrared thermometer. The quality of graphene was checked by LEED and STM [14]. The Mg atoms were evaporated out from a water-cooled Knudsen cell evaporator and deposited on the graphene surface at room temperature (RT). The deposition rate of Mg is about 0.2 monolayer·min^{-1}. After 30 min deposition, the sample was annealed at 280 °C to intercalate the Mg atoms underneath the graphene. Owing to the desorption of Mg atoms during annealing, the amount of intercalated Mg is smaller than that originally deposited. A few cycles of deposition and annealing are needed for more Mg intercalation. The final thickness of intercalated Mg film is controlled by the total deposition time. Oxygen was supplied in molecular form via a leak valve. The sample was exposed to oxygen with a pressure of 2.0×10^{-3} Pa at 280 °C to oxidize Mg. Then we raised the annealing temperature to crystallize magnesium oxide. The amorphous MgO becomes crystalline at 430 °C. The thickness of MgO layer is determined by that of intercalated Mg. The growth process is schematically illustrated in Fig. 1a–d. Each step of the sample growth process was monitored by LEED. The sample was transferred in situ to an Omicron UHV-LT-STM system to characterize the microscopic structure. XPS was performed in a ThermoFisher Scientific ESCALAB 250X system (Monochromatic Al Kα source, 1486.6 eV) to study the chemical state of magnesium. The cross-sectional sample was studied using an aberration-corrected STEM operated at 60 kV to confirm the structure and thickness of the intercalated MgO layer.

Figure 1e is a typical LEED pattern of graphene on Ru(0001) surface, consisting of six groups of spots. The inner and outer spots in each group, indicated by the dashed and solid arrows, originate from the Ru(0001) lattice and graphene adlayer, respectively. The additional satellite spots surrounding the Ru spots in a hexagonal pattern signify the moiré superstructure of graphene on Ru(0001) surface. The corresponding STM images show that graphene is corrugated on Ru(0001) surface because of lattice mismatch, which is similar to previous reports [14]. After Mg intercalation, we found that a 2×2 superstructure emerged on the sample as shown in the LEED pattern in Fig. 1f. This well-ordered superstructure has a period of 0.54 nm, twice the lattice constant of the Ru(0001) surface. The superstructure in our sample is different from the 5×5 or 7×7 Mg structure on Ru(0001) reported previously [25]. If we deposit Mg on pure Ru(0001) without graphene, the 2×2 structure could also be observed in LEED pattern (Fig. S1). Therefore, although this 2×2 structure is not clear and need further investigation, we can confirm that it is a structure induced by Mg and Ru. The superstructure indicates that Mg is indeed intercalated between graphene and Ru(0001) substrate. In addition, the original moiré pattern of graphene becomes hazy. It could be interpreted that the 2×2 superstructure resulting from the intercalated Mg weakens the graphene–Ru interaction and leads to the blurred moiré pattern.

Figure 1g is the LEED pattern of the oxidized sample, where the 2×2 superstructure spots disappear and leave only graphene diffraction spots after oxidation. This result and XPS result (shown below) indicate that magnesium has been oxidized. And, the oxide is amorphous due to the absence of MgO diffraction spots. Moreover, because the

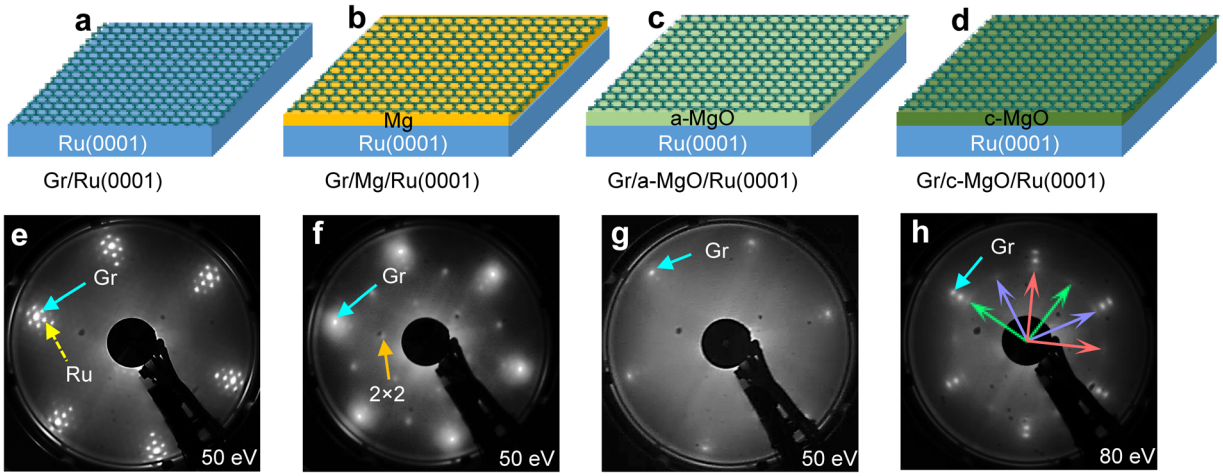

Fig. 1 Schematic illustrations and LEED patterns of Mg intercalation and oxidation process between graphene and Ru(0001) substrate: **a** graphene formation on Ru(0001); **b** Mg intercalation after Mg deposition and annealing; **c** Mg oxidation by exposing sample to O_2 at 280 °C, where amorphous magnesium oxide (a-MgO) is formed; **d** amorphous magnesium oxide transforming into crystalline magnesium oxide (c-MgO) by further annealing at high temperature; LEED patterns of **e** Gr/Ru(0001), **f** Gr/Mg/Ru(0001), **g** Gr/a-MgO/Ru(0001), and **h** Gr/c-MgO/Ru(0001), where graphene is abbreviated as Gr, and red, purple and green arrows indicate three domains of MgO(001) plane on hexagonal Ru(0001), respectively

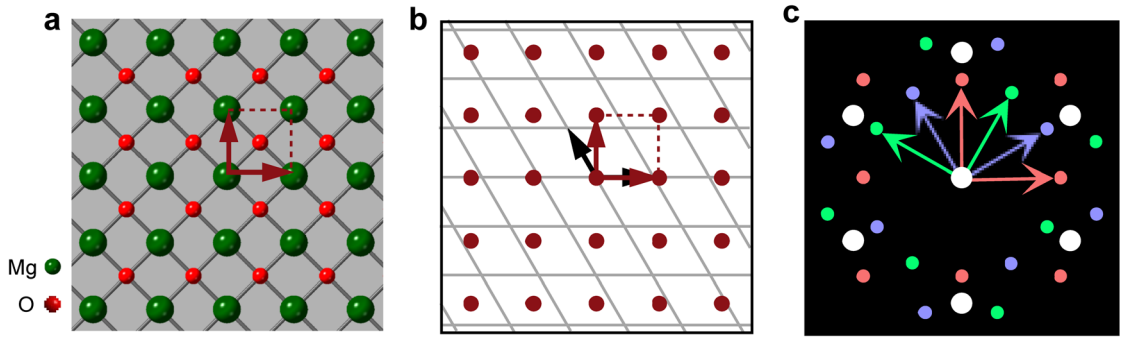

Fig. 2 Structure analysis of crystalline MgO on Ru(0001): **a** structure model of MgO(001) plane, where green and red balls represent magnesium and oxygen atoms, respectively, and square composed of arrows and dashed lines represents unit cell; **b** schematic illustration of one representative domain of two-dimensional lattice of MgO(001) plane (red dots) on Ru(0001) surface (gray grid) without graphene, where square is the same with that in **a**; **c** simulated LEED pattern of c-MgO/Ru(0001), where green, purple, and red arrows represent basis vectors of different domains in reciprocal space, white spots represent diffraction spots of Ru(0001), and the colored spots are those from MgO(001) surface of the three different domains

diffraction spots of Ru is fuzzy, there must be something between graphene and Ru(0001). The survey scan of XPS spectrum shows that there are only C, O, Mg and Ru in the sample (Fig. S2). So, the materials between graphene and Ru(0001) is amorphous MgO (a-MgO). Our result is consistent with the reported result that oxygen exposure causes the preferential intercalation rather than etching of graphene under a similar experimental condition [26].

After we obtained the Gr/a-MgO/Ru(0001) sample, we slowly increased the annealing temperature to 430 °C. Finally, a well-defined structure appeared in the LEED pattern, as displayed in Fig. 1h. This structure consists of square lattice which is incommensurate with the Ru(0001) substrate. There are three domains according to the LEED results, which are marked by green, purple and red arrows in Fig. 1h. Based on the lattice constant of Ru(0001) surface, we estimate that the in-plane lattice constant of the square structure is about 0.3004 nm, in good agreement with the value of MgO(001) surface, which is 0.2978 nm. LEED patterns measured at different regions of the sample surface remain unchanged, indicating that graphene and MgO layers extend over the entire Ru substrate (Fig. S3).

To further understand the structure of crystalline MgO (c-MgO), we simulated and analyzed the structure. Figure 2a is a structure model of MgO(001) plane. Figure 2b schematically shows the lattice relationship of MgO(001) plane on Ru(0001). Using the LEED analyzing software LEEDpat (version 4.1), we establish an incommensurate square lattice on Ru(0001) using the known lattice constants. After considering all three domains, we get a

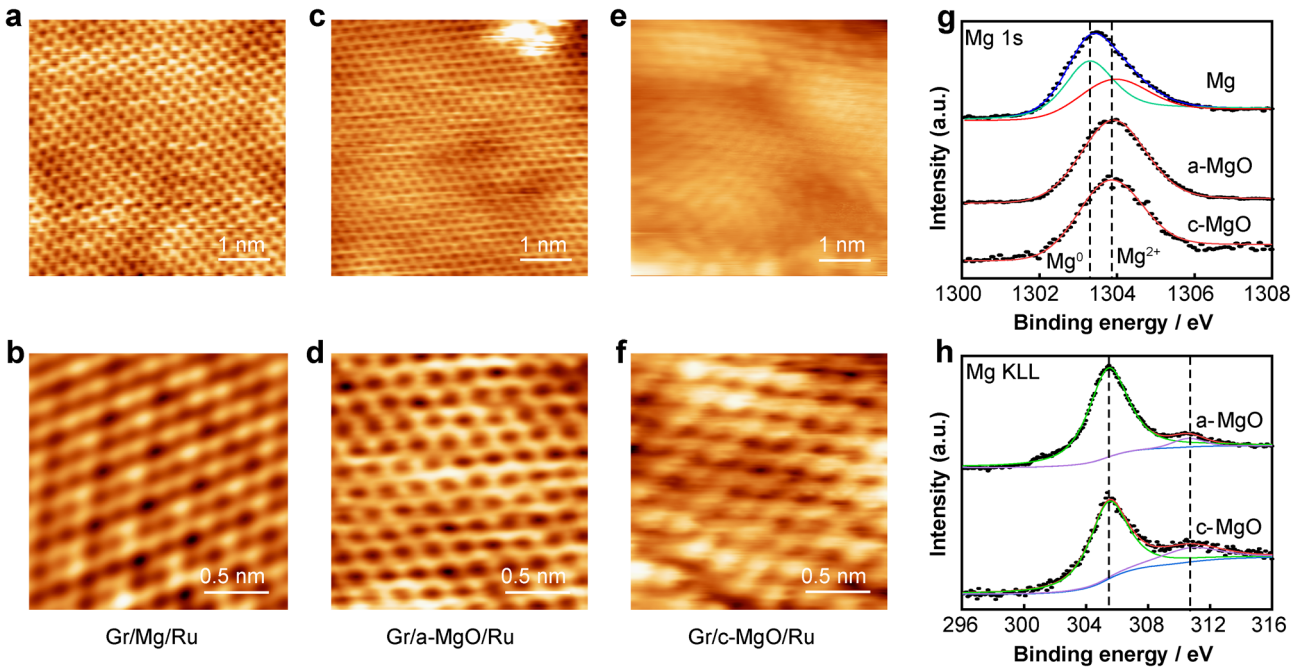

Fig. 3 STM images of graphene on Ru(0001) with **a**, **b** Mg, **c**, **d** amorphous MgO and **e**, **f** crystalline MgO intercalation with scanning parameters of 0.5 nA@-1 V, 3 nA@-40 mV, 0.4 nA@-700 mV, 3 nA@-30 mV, 2 nA@-20 mV, and 2 nA@-100 mV, respectively; **g** XPS measurements for Gr/Mg/Ru, Gr/a-MgO/Ru, and Gr/c-MgO/Ru samples with binding energies close to Mg 1s electrons, revealing that Mg chemical state changes from Mg^0 to Mg^{2+}, and Mg has been completely oxidized; **h** X-ray excited Auger electron spectra (XAES) of Mg $KL_{2,3}L_{2,3}$ of amorphous MgO intercalated sample (upper panel) and crystalline MgO intercalated sample (lower panel), where small shoulder at about 301 eV in upper panel probably originates from metallic Mg that has not been oxidized, green peaks demonstrate Mg oxide, and purple lines are satellite peaks which come from MgO [32, 33]

simulated LEED pattern (Fig. 2c), in which the inner (10) and (01) diffraction spots are completely consistent with our experimental results (Fig. 1h). The 12-fold symmetry of the diffraction spots is due to the fourfold symmetry of MgO(001) plane and the sixfold symmetry of Ru(0001) substrate. We noticed that, in our LEED experimental image in Fig. 1h, the second-order diffraction points (11) are not visible. This is because the diffraction intensities of different points like (10) and (11) of MgO(001) plane vary differently with incident electron energy [27], which induces that the second-order (11) diffraction spots do not appear in some case due to the selection of incident electron energy [28].

STM was employed to characterize the surface morphology of the samples at each stage. After Mg intercalation, graphene becomes uniform and flat (Fig. 3a). Figure 3b is a zoom-in STM image of the Gr/Mg/Ru sample, which displays a 2 × 2 superstructure caused by intercalated Mg layer, in agreement with the LEED pattern in Fig. 1f. This 2 × 2 superstructure may originate from the intercalated Mg itself or Mg–Ru compounds. The absence of an obvious 2 × 2 superstructure in the large-scale image (Fig. 3a) may be due to the large tip-sample distance determined by the scanning conditions. The STM images of the graphene sample intercalated with amorphous MgO are shown in Fig. 3c, d. In agreement with the LEED pattern, the 2 × 2 superstructure vanishes due to oxidation and the atomic resolution image demonstrates clearly the intact graphene honeycomb lattice. STM was also used to probe the crystalline-MgO intercalated sample, and the results, as shown in Fig. 3e, f, indicate that graphene is continuous, although the MgO underneath is not so flat. Furthermore, we find the single atom vacancy in graphene after MgO intercalation has the triangular interference pattern and the fast Fourier transform (FFT) of the corresponding STM image shows $\sqrt{3} \times \sqrt{3}$ $R30°$ pattern (Fig. S4). This indicates that graphene has decoupled from the Ru(0001) substrate [29, 30].

XPS was applied to further characterize the chemical environment of magnesium. Figure 3g shows the characteristic XPS spectra from the core level of Mg 1s for Mg, a-MgO and c-MgO intercalated samples. The reason why we select Mg 1s instead of Mg 2p is that the binding energy of Mg 2p overlaps with that of Ru 4p. Before oxygen intercalation, the Mg 1s spectrum is composed of two peaks. They are located at binding energies of 1303.3 and 1303.9 eV, corresponding to the characteristic signals of Mg-Mg peak (colored in cyan) and Mg–O peak (colored in red), respectively [31]. After oxidation, the experimental XPS spectra could be fitted well with a single peak (colored

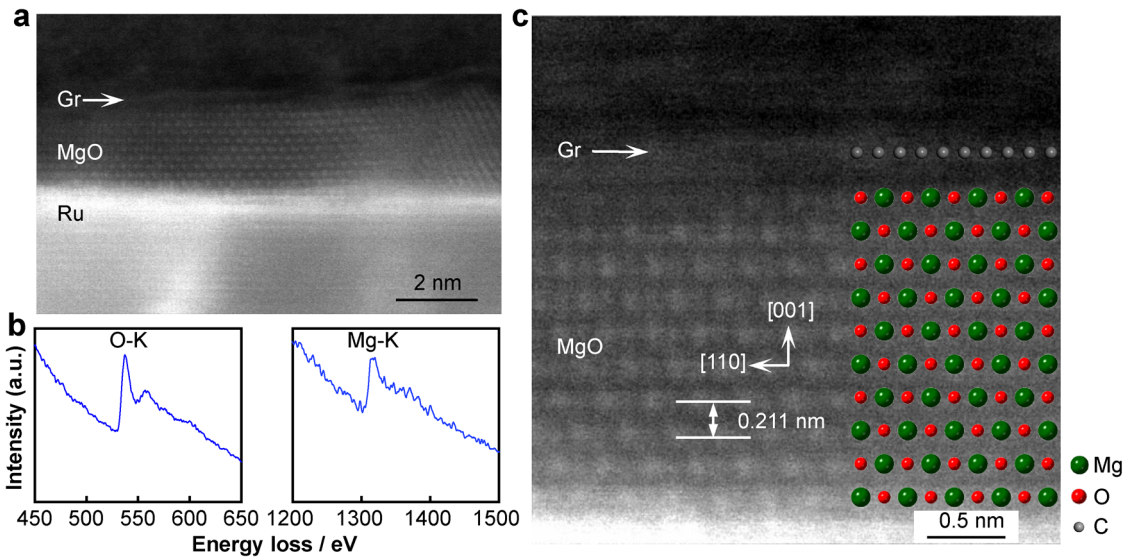

Fig. 4 Annular dark field (ADF) STEM images and EELS of Gr/c-MgO/Ru sample, showing atomically resolved MgO intercalation layer between graphene and Ru(0001): **a** STEM image revealing formation of MgO beneath graphene; **b** EELS spectra of MgO intercalation layer; **c** high-resolution STEM image of Gr/c-MgO/Ru sample, where green, red and gray balls represent magnesium, oxygen and carbon atoms, respectively

in red) located at the binding energy of 1303.9 eV for both MgO-intercalated samples, corresponding to the characteristic signals of Mg–O peak [31] (detailed oxidation process is shown in Fig. S5). The X-ray excited Auger electron spectra (XAES) of Mg $KL_{2,3}L_{2,3}$ shown in Fig. 3h include two peaks, which clearly demonstrates that the Mg has been completely oxidized [32]. XPS results indicate that the intercalated magnesium has been fully oxidized and we successfully fabricated graphene on an oxide substrate by intercalation and oxidation.

To further confirm the structure and thickness of the intercalated MgO layer, we performed cross-sectional STEM study. Figure 4a shows an annular dark field (ADF) STEM image of the Gr/c-MgO/Ru sample in cross-sectional view, which shows the formation of $\sim$ 2.3-nm-thick crystalline MgO between graphene and Ru substrate. Electron energy loss spectroscopy (EELS) measurement confirms that the intercalation layer is composed of Mg and O, and the spectra of Mg–K and O–K, shown in Fig. 4b, demonstrate that Mg has been oxidized. Although the sample is not homogeneous and there are regions with thinner crystalline MgO (not shown here), we demonstrate that the thickness of the oxide intercalation layer between graphene and metal substrate could be further promoted, from 1.8 nm in Ref. [21] to 2.3 nm we achieved here. Figure 4c shows the atomic-resolution STEM image of the crystalline MgO intercalation layer, with the rock salt MgO structural model overlaid. The MgO crystal orientation is also displayed in Fig. 4c, and the out-of-plane orientation is [001]. From the results of STEM, it can be confirmed that the structure and the crystal orientation of intercalated MgO layer inferred by LEED are correct. A grain boundary is also observed in the right part of Fig. 4a. After intercalation of crystalline MgO, graphene layer could be observed distinctly on top of MgO in the STEM images, as demonstrated in Fig. 4a, c, which agrees with STM results in Fig. 3e, f. By STEM characterizations, we can also estimate that the MgO domain size is several to tens of nanometers. The grain boundaries between the domains may introduce stress in graphene.

Since MgO is an insulator with a band gap of about 7.8 eV, our work demonstrates a transfer-free fabrication of high-quality large-area graphene on such dielectric materials. In addition, graphene is an excellent material for spintronics with large spin relaxation length (larger than several micrometers) [34] and MgO is an efficient tunnel barrier material for spin injection [35]. The combination of graphene and MgO, thus, holds promising applications in novel spintronic devices, such as spin valves [24]. However, direct deposition of MgO on graphene by sputtering will destroy the graphene layer. Our work provides a new route to construct graphene and its tunnel barrier, which may be used in spintronic devices.

In summary, using LEED, STM, XPS and STEM, we have studied Mg intercalation and further oxidation between graphene and Ru(0001). The deposited Mg atoms intercalate into the graphene/Ru interface and form 2×2 superstructure when the sample is annealed at 280 °C. The magnesium could be oxidized by exposing the sample to oxygen and annealing. The morphology of intercalated MgO can be controlled using different annealing temperatures, amorphous at 280 °C and crystalline at 430 °C, as

verified by LEED. XPS characterization indicates that the intercalated Mg could be completely oxidized. STEM results show that the crystalline MgO intercalation layer has a rock salt structure and its thickness is up to ~ 2.3 nm. Our work provides a new method to fabricate graphene/MgO/metal heterostructures by intercalating and oxidizing Mg underneath graphene, which may have potential applications in microelectronic devices based on high quality graphene.

Acknowledgements This study was financially supported by the National Key Research & Development Program of China (Nos. 2019YFA0308500, 2018YFA0305800 and 2016YFA0202300), the National Natural Science Foundation of China (Nos. 61888102 and 61925111), the Strategic Priority Research Program of Chinese Academy of Sciences (Nos. XDB30000000 and XDB28000000), and the CAS Key Laboratory of Vacuum Physics.

References

[1] Novoselov KS, Geim AK, Morozov SV, Jiang D, Zhang Y, Dubonos SV, Grigorieva IV, Firsov AA. Electric field effect in atomically thin carbon films. Science. 2004;306(5696):666.
[2] Novoselov KS, Jiang D, Schedin F, Booth TJ, Khotkevich VV, Morozov SV, Geim AK. Two-dimensional atomic crystals. Proc Natl Acad Sci USA. 2005;102(30):10451.
[3] Su CY, Lu AY, Xu YP, Chen FR, Khlobystov AN, Li LJ. High-quality thin graphene films from fast electrochemical exfoliation. ACS Nano. 2011;5(3):2332.
[4] Li XS, Cai WW, An JH, Kim S, Nah J, Yang DX, Piner R, Velamakanni A, Jung I, Tutuc E, Banerjee SK, Colombo L, Ruoff RS. Large-area synthesis of high-quality and uniform graphene films on copper foils. Science. 2009;324(5932):1312.
[5] Chen XD, Liu ZB, Zheng CY, Xing F, Yan XQ, Chen YS, Tian JG. High-quality and efficient transfer of large-area graphene films onto different substrates. Carbon. 2013;56:271.
[6] Yan C, Cho JH, Ahn JH. Graphene-based flexible and stretchable thin film transistors. Nanoscale. 2012;4(16):4870.
[7] Wang DY, Huang IS, Ho PH, Li SS, Yeh YC, Wang DW, Chen WL, Lee YY, Chang YM, Chen CC, Liang CT, Chen CW. Clean-lifting transfer of large-area residual-free graphene films. Adv Mater. 2013;25(32):4521.
[8] Pan GH, Li B, Heath M, Horsell D, Wears ML, Al Taan L, Alwan S. Transfer-free growth of graphene on SiO_2 insulator substrate from sputtered carbon and nickel films. Carbon. 2013;65:349.
[9] Yang W, Chen GR, Shi ZW, Liu CC, Zhang LC, Xie GB, Cheng M, Wang DM, Yang R, Shi DX, Watanabe K, Taniguchi T, Yao YG, Zhang YB, Zhang GY. Epitaxial growth of single-domain graphene on hexagonal boron nitride. Nat Mater. 2013;12(9):792.
[10] Lippert G, Dabrowski J, Lemme M, Marcus C, Seifarth O, Lupina G. Direct graphene growth on insulator. Phys Status Solidi B. 2011;248(11):2619.
[11] Wei DP, Mitchell JI, Tansarawiput C, Nam W, Qi MH, Ye PD, Xu XF. Laser direct synthesis of graphene on quartz. Carbon. 2013;53:374.
[12] Rummeli MH, Bachmatiuk A, Scott A, Borrnert F, Warner JH, Hoffman V, Lin JH, Cuniberti G, Buchner B. Direct low-temperature nanographene cvd synthesis over a dielectric insulator. ACS Nano. 2010;4(7):4206.
[13] Guo H, Chen H, Que YD, Zheng Q, Zhang YY, Bao LH, Huang L, Wang YL, Du SX, Gao HJ. Low-temperature growth of large-scale, single-crystalline graphene on Ir(111). Chin Phys B. 2019;28(5):056107.
[14] Pan Y, Zhang HG, Shi DX, Sun JT, Du SX, Liu F, Gao HJ. Highly ordered, millimeter-scale, continuous, single-crystalline graphene monolayer formed on Ru (0001). Adv Mater. 2009;21(27):2777.
[15] Xu XZ, Zhang ZH, Dong JC, Yi D, Niu JJ, Wu MH, Lin L, Yin RK, Li MQ, Zhou JY, Wang SX, Sun JL, Duan XJ, Gao P, Jiang Y, Wu XS, Peng HL, Ruoff RS, Liu ZF, Yu DP, Wang EG, Ding F, Liu KH. Ultrafast epitaxial growth of metre-sized single-crystal graphene on industrial Cu foil. Sci Bull. 2017;62(15):1074.
[16] Huang L, Pan Y, Pan LD, Gao M, Xu WY, Que YD, Zhou HT, Wang YL, Du SX, Gao HJ. Intercalation of metal islands and films at the interface of epitaxially grown graphene and Ru(0001) surfaces. Appl Phys Lett. 2011;99(16):163107.
[17] Mao JH, Huang L, Pan Y, Gao M, He JF, Zhou HT, Guo HM, Tian Y, Zou Q, Zhang LZ, Zhang HG, Wang YL, Du SX, Zhou XJ, Castro Neto AH, Gao HJ. Silicon layer intercalation of centimeter-scale, epitaxially grown monolayer graphene on Ru(0001). Appl Phys Lett. 2012;100(9):093101.
[18] Li LF, Wang YL, Meng L, Wu RT, Gao HJ. Hafnium intercalation between epitaxial graphene and Ir(111) substrate. Appl Phys Lett. 2013;102(9):093106.
[19] Fei XM, Zhang LZ, Xiao WD, Chen H, Que YD, Liu LW, Yang K, Du SX, Gao HJ. Structural and electronic properties of Pb—intercalated graphene on Ru(0001). J Phys Chem C. 2015;119(18):9839.
[20] Enderlein C, Kim YS, Bostwick A, Rotenberg E, Horn K. The formation of an energy gap in graphene on ruthenium by controlling the interface. New J Phys. 2010;12(3):033014.
[21] Lizzit S, Larciprete R, Lacovig P, Dalmiglio M, Orlando F, Baraldi A, Gammelgaard L, Barreto L, Bianchi M, Perkins E, Hofmann P. Transfer-free electrical insulation of epitaxial graphene from its metal substrate. Nano Lett. 2012;12(9):4503.
[22] Wang XY, Guo H, Lu JC, Lu HL, Lin X, Shen CM, Bao LH, Du SX, Gao HJ. Intercalation of germanium oxide beneath large-area and highquality epitaxial graphene on Ir(111) substrate. Chin Phys B. 2021;30(4):048102.
[23] Omiciuolo L, Hernandez ER, Miniussi E, Orlando F, Lacovig P, Lizzit S, Menteş TO, Locatelli A, Larciprete R, Bianchi M, Ulstrup S, Hofmann P, Alfè D, Baraldi A. Bottom-up approach for the low-cost synthesis of graphene-alumina nanosheet interfaces using bimetallic alloys. Nat Commun. 2014;5(1):5062.
[24] Liu YP, Idzuchi H, Fukuma Y, Rousseau O, Otani Y, Lew WS. Spin injection properties in trilayer graphene lateral spin valves. Appl Phys Lett. 2013;102(3):033105.
[25] Herranz T, Santos B, McCarty KF, de la Figuera J. Real-space study of the growth of magnesium on ruthenium. Surf Sci. 2011;605(9):903.
[26] Sutter P, Sadowski JT, Sutter EA. Chemistry under cover: tuning metal-graphene interaction by reactive intercalation. J Am Chem Soc. 2010;132(23):8175.
[27] Urano T, Kanaji T. Surface structure of MgO(001) surface studied by LEED. Surf Sci. 1983;134(1):109.
[28] Ahmad SS, He W, Zhang YS, Tang J, Gul Q, Zhang XQ, Cheng ZH. Effect of Cu buffer layer on magnetic anisotropy of cobalt thin films deposited on MgO(001) substrate. AIP Adv. 2016;6(11):115101.
[29] Ma YC, Lehtinen PO, Foster AS, Nieminen RM. Magnetic properties of vacancies in graphene and single-walled carbon nanotubes. New J Phys. 2004;6:68.

[30] Mao JH, Jiang YH, Moldovan D, Li GH, Watanabe K, Taniguchi T, Masir MR, Peeters FM, Andrei EY. Realization of a tunable artificial atom at a supercritically charged vacancy in graphene. Nat Phys. 2016;12(6):545.
[31] Li J, Jiang YZ, Li Y, Yang DR, Xu YB, Yan M. Origin of room temperature ferromagnetism in MgO films. Appl Phys Lett. 2013;102(7):072406.
[32] Asami K, Ono S. Quantitative X-ray photoelectron spectroscopy characterization of magnesium oxidized in air. J Electrochem Soc. 2000;147(4):1408.
[33] Chambers SA, Tran TT. Core-level binding energies and photoelectron diffraction in cleaved and homoepitaxial MgO(100). Surf Sci Spectra. 1998;5(3):203.
[34] Tombros N, Jozsa C, Popinciuc M, Jonkman HT, van Wees BJ. Electronic spin transport and spin precession in single graphene layers at room temperature. Nature. 2007;448(7153):571.
[35] Wang WH, Pi K, Li Y, Chiang YF, Wei P, Shi J, Kawakami RK. Magnetotransport properties of mesoscopic graphite spin valves. Phys Rev B. 2008;77(2):020402.